

**REDOX DYNAMICS IN SILICATE MELTS: THE SEMICONDUCTOR CONDITION AND ITS IMPACT ON TEXTURE.** Reid F. Cooper, Department of Geological Sciences, Brown University, Providence, RI 02012–1846 USA (Reid\_Cooper@Brown.edu).

**Introduction:** Transition-metal-cation redox experiments designed to characterize the rate of oxygen-species diffusion in silicate melts reveal a startling result: for melts of similar polymerization, chemical diffusion seems to occur some  $10^2$ – $10^3$  times faster than that seen for  $^{18}\text{O}$  in tracer diffusion experiments [1–3]. The primary reason for the discrepancy is that, in many cases, the chemical diffusion producing the valence-state change of transition-metal cations does not involve diffusion of an oxygen species at all, but rather is wrought by the diffusion of network-modifying cations whose motion is decoupled from that of other ions by the high transport coefficient of electronic defects, i.e., electron holes in the valence band ( $h^\bullet$ ) and/or electrons in the conduction band ( $e'$ )—a situation known as the “semiconductor condition” in chemical kinetics [4]. Cation-diffusion-effected redox reactions, in both melts and minerals, create textures with implications, e.g., for the perceived chemistry of planetary surfaces and for the structures of metal-bearing chondrules.

**Oxidation of basaltic magmas:** Ion backscattering spectrometry proves unequivocally (i.e., the texture is

unique) that the physical process of oxidation of a basaltic liquid occurs, for anhydrous conditions, according to the dynamic shown in Fig. 1a [5]. When the external oxygen fugacity ( $f_{\text{O}_2}$ ) exceeds the magnetite-hematite (MH) buffer, two internal reaction fronts move into the melt:  $\xi'''$  is the location where the local  $f_{\text{O}_2}$  finally sees the melt go subliquidus, and magnetite nucleates;  $\xi''$  is the MH buffer, where the magnetite formed in the first (crystallization) reaction is converted to hematite. The process is accomplished by the flux ( $j_i$ ) of network-modifier  $\text{Fe}^{2+}$  and  $\text{Ca}^{2+}$  to the free surface, where they form thin-film oxides that coat the surface. The cation flux is charge-compensated by a counterflux of  $h^\bullet$ . For  $f_{\text{O}_2}$  conditions lower than MH but sufficiently high to intersect the liquidus, only the single reaction front  $\xi'''$  moved into the melt, and very little  $\text{Ca}^{2+}$  is mobilized; thus  $x$  in the figure approaches unity and  $y \ll x$ . The thin-film oxide is seen naturally as the multicolored specular patina on fresh basalt flows [e.g., 6], the color variation being a function of the film thickness. Reflectance spectroscopy on these surfaces clearly would reveal a  $\text{Fe}^{2+,3+}$  content exceeding greatly that of the bulk magma. The cation-diffusion-dominated oxidation response was proven to occur for  $\text{Fe}^{2+,3+}$  concentrations as low as 0.04 at% [7]. The model has applicability to a variety of phenomena, including the oxidation of  $\text{Fe}^{2+}$ -bearing rocks and minerals at low-temperatures [e.g., 8, 9]. For terrestrial basaltic compositions, low-temperature oxidation sees mobilization of alkali ions—their transport coefficients (product of concentration and mobility) exceeding those of the alkaline earths at low temperature.

**Reduction of iron-oxide-bearing melts:** Experiments on  $\text{Fe}^{2+}$ -bearing magnesium aluminosilicate (Fe-MAS) melts demonstrated the reduction dynamic depicted in Fig. 1b [10]: oxygen chemically ablates from the free surface and network-modifying cations diffuse inward, charge-compensated by a counterflux of  $h^\bullet$ . The textures are dramatic: single crystals of  $\alpha$ -Fe form at the free surface,  $\xi'$ , showing a preferential  $\{111\}$  interface with the environment (Fig. 2a); nm-scale crystals of  $\alpha$ -Fe nucleate at an internal front,  $\xi''$  (Fig. 2b). Dispersal of the internal iron grains as a “string of pearls” suggests that the initial silicate melt structure includes percolation of network modifiers. Surface iron crystals are affected by vapor-phase transport of iron.

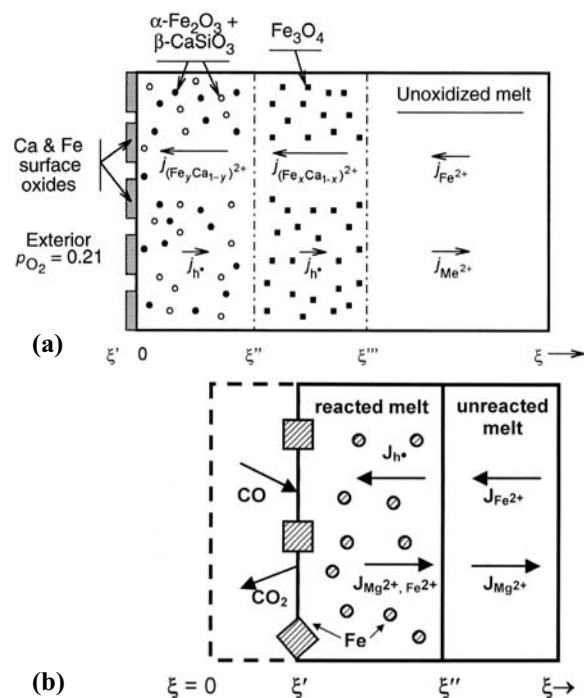


**Figure 1.** Redox dynamics in  $\text{Fe}^{2+,3+}$ -bearing silicate melts. **(a)** Oxidation in a basaltic melt. **(b)** Reduction in an Fe-MAS melt. Cation-diffusion-effected reactions are possible because of the flux of electron holes.

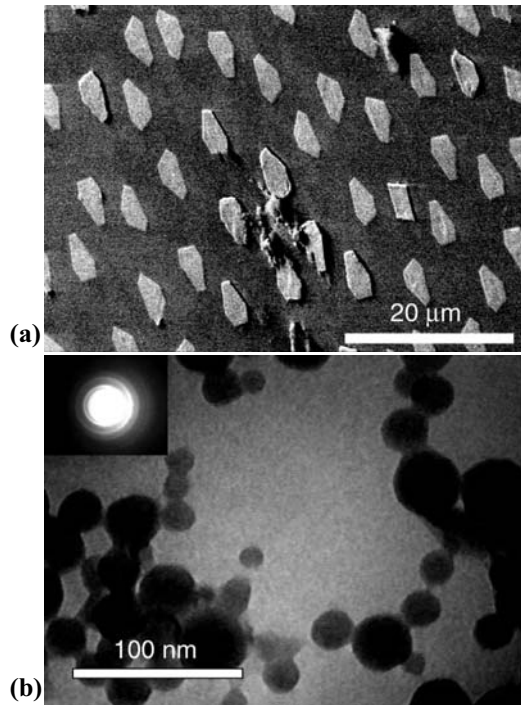


**Figure 2.** Reduction microstructure for a FeMAS melt partially transformed to  $\text{Fe}^0$  plus MAS melt. (1355°C, 1/2h, QIF-2). (a) SEI of the free surface of the quenched droplet: crystals are  $\alpha\text{-Fe}$ , most showing  $\{111\}$  planes with  $\{100\}$  truncations. (b) TEM image and HEED pattern (inset) for the specimen between the free surface and  $\zeta''$ : the nm-scale, subspherical particles are  $\alpha\text{-Fe}$ .

The reduction dynamic in which inward diffusion of cations, charge-compensated by a flux of electronic defects, sees metal precipitates form at an internal interface has been demonstrated as active in the reduction of transition-metal cation-bearing crystalline oxides [11]; inevitably, this is the mechanism involved in the formation of “dusty” olivine seen in reduced chondrules [e.g., 12].

Because the transport coefficients are different for all component ions in a silicate melt, and because electronic defects can decouple fluxes, redox dynamics produce surface chemistries that are far from equilibrium. Consider the ion-backscattering spectra for quenched melt specimens of an  $\text{Fe}^{2+}$ -bearing calcium magnesium aluminosilicate (Fe-CMAS) melt (Fig. 3): the chemical profile seen is consistent with a dynamic similar to that shown in Fig. 1b; the profile is in no way consistent with a standard evaporation process [13]. The reaction dynamic produces a surface chemistry that is enriched in  $\text{SiO}_2$ ,  $\text{MgO}$  and  $\text{CaO}$ .

We have pursued no formal reduction studies of alkali-oxide-bearing silicate melts, but lessons learned in the oxidation of basalt liquids and glasses can inform speculation. Despite the higher mobility of the alkali network modifiers in silicate melts, their concen-

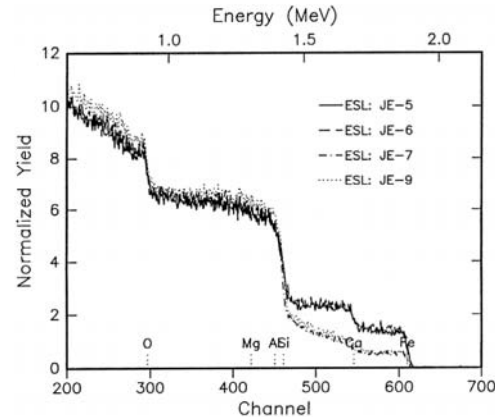


**Figure 3.** 2.0MeV ion ( $^4\text{He}^{2+}$ )-backscattering spectra for Fe-CMAS melts (composition “JE,” a model basalt) processed by electrostatic levitation (ESL). Specimens JE-5 (1550°C) and JE-6 (1500°C) were levitated and melted at  $f_{\text{O}_2}\sim\text{QIF}+1$ ; these spectra show essentially unreacted melt: the spectra indicate that the melt composition is uniform with depth. Specimens JE-7 (1550°C) and JE-9 (1650°C) were levitated and melted at  $f_{\text{O}_2}\sim\text{QIF}-0.5$ ; these spectra are consistent with rapid inward diffusion of  $\text{Fe}^{2+}$  and less-rapid inward diffusion of  $\text{Ca}^{2+}$ . The concentration profiles for  $\text{Ca}^{2+}$  seen between the Ca and Si edges, combined with the increase in backscattering yield at energies below the Si edge, are inconsistent with an evaporation process. The reduction dynamic results in a quenched-melt surface enriched in  $\text{SiO}_2$ ,  $\text{MgO}$  and  $\text{CaO}$ .

tration is lower than the alkaline earths and, too, their “potency” in an electron-exchange reaction is but half that of the alkaline earths. Reduction at high temperature, thus, should increase the concentration of alkali cations near the free surface of the melt, affecting processes, e.g., like evaporation and/or the presence and chemistry of surface films that are often attributed to condensation.

**References:** [1] Dunn T. (1986) In *Silicate Melts*, Mineral. Soc. Canada, pp. 57-92. [2] Cook G.B. et al. (1990) *J. Non-Crys. Solids*, 120, 207-222. [3] Chakraborty S. (1995) *RiMG*, 32, 411-503. [4] Schmalzried H. (1981) *Solid State Reactions (2<sup>nd</sup> Edition)*, Verlag Chemie, p.99. [5] Cooper R.F. et al. (1996) *Science*, 274, 1173-1176. [6] Dutton C.E. (1884) In *USGS 4<sup>th</sup> Annual Report*, pp.75-219. [7] Cook G.B. and Cooper R.F. (2000) *Am. Mineral.*, 85, 397-406. [8] Minitti M.E. et al. (2002) *JGR*, 107, doi:10.1029/2001JE001518. [9] Cooper R.F. et al. (1996) *GCA*, 60, 3253-3265. [10] Everman R.L.A. and Cooper R.F. (2003) *J. Am. Ceram. Soc.*, 86, 487-494. [11] Schmalzried H. (1984) *Ber. Bunsenges. Phys. Chem.*, 88, 1186-1191. [12] Leroux H. et al. (2003) *Meteor. Planet. Sci.*, 38, 81-94. [13] Cooper R.F. (1996) *Proc. SPIE*, 2809, 69-77.